Comparison of Nickel Methanesulfonate and Nickel Sulfamate Electrolytes

By Nicholas M. Martyak and Robert Seefeldt*

Nickel sulfamate plating solutions are used to deposit a low stress coating but the electrolyte has a small operating window with regards to pH, temperature and anode material. Nickel methanesulfonate, $Ni(CH_3SO_3)_2$ electrolytes are an alternative to producing a coating with similar deposit structures and properties. Electrochemical investigations show that methanesulfonate solutions follow a similar reduction mechanism but inhibition of nickel-ion reduction caused by the sulfamate anion is not as apparent in the methanesulfonate electrolyte. SEM images show epitaxial growth of thin nickel coatings on copper governed by an instantaneous growth process. Slightly thicker nickel deposits follow a progressive growth mechanism leading to grain coalescence and growth.

Nickel sulfamate plating has been extensively used during the past forty to fifty years in electroforming processes where engineering coatings require a low stress deposit.[1-3] In addition to the low stress, these coatings usually exhibit good ductility. However, the composition of the nickel sulfamate electrolyte (Ni^{+2} concentration, organic additives) and deposition conditions (pH, temperature, anode material, etc.) can affect the porosity, hardness, coefficient of thermal expansion and tensile strength, among other mechanical properties. For example, Kaja, *et.al.*[4] showed that the efficiency for nickel ion reduction was strongly influenced by the pH as was the grain size of the nickel deposit.

Nuts & Bolts: What This Paper Means to You

Nickel sulfamate solutions have been the mainstay in electroforming applications for decades. Here, an alternative emerges, building on the work presented by the authors last month. The nickel methanesulfonate process is compared to the traditional sulfamate process and is shown to possess advantages in operation as well as deposit structural growth.

One of the major drawbacks to the sulfamate electrolyte is the instability of the $NH_2SO_3^-$ anion. The hydrolysis of sulfamate occurs according to:[5]

$$H_2NSO_2O^- + H_3O^+ \rightarrow NH_4^+ + HSO_4^- \rightarrow SO_4^{-2} + H_3O^+$$

Huang[6] showed that hydrolysis of sulfamate increased with an increase in acidity, temperature and anode current density. Jiazhu and co-workers,[7] using differential pulse polarography and Raman spectroscopy, identified dithionate, $S_2O_6^{-2}$ as a possible decomposition product.

Because of the small operating window for nickel sulfamate, a new electrolyte is warranted that can produce similar deposit properties yet can be used at low pH values and higher temperatures to increase the deposition rates. Recently, Martyak[8] and Kudryavtsev. *et.al.*[9] showed that nickel methanesulfonate, $Ni(CH_3SO_3)_2$ solutions may be a viable alternative to the sulfamate process. Methanesulfonate (MSA) is a stable anion that does not decompose even at temperatures of about 100°C (212°F)[10] and allows for the use of insoluble anodes.

This study investigates the use of MSA as a new acid electrolyte for the deposition of low-stress nickel. Electrochemical studies were done to compare the deposition of nickel from the MSA and sulfamate solutions. Scanning electron microscopy (SEM) and x-ray diffractometry (XRD) were done to compare deposit morphologies and crystallographic structures.

Experimental procedures

Nickel methanesulfonate solutions were prepared by dissolving nickel carbonate and commercially available methanesulfonic acid, CH_3SO_3H into doubly distilled water. Commercially available nickel sulfamate was also used. The final Ni^{+2} concentration was 77 g/L (10.3 oz/gal) in both electrolytes and 6.0 g/L (0.8 oz/gal) nickel chloride

* *Corresponding author:*
Nicholas M. Martyak
ATOFINA Chemicals, Inc.
Division of Thio and Fine Chemicals
900 First Avenue
King of Prussia, PA 19406
E-mail: nick.martyak@atofina.com

was added to increase anode corrosion. Boric acid was used at 35 g/L (4.7 oz/gal) as a buffer and both solutions contained a non-ionic wetting agent. The solutions were adjusted to pH 3.8, filtered and heated to 50°C (122°F) during testing.

Electrochemical studies were done using a potentiostat** and all potentials were recorded versus a saturated calomel electrode (SCE). Polarization measurements were made using a platinum working and an iridium-coated titanium oxide counter electrode at 2 mV/sec. Cyclic voltammetric measurements were performed from 0 to $-0.8V_{SCE}$ stopping the scan at pre-selected negative voltages. Potential-step measurements were made on the various solutions by stepping the potential from –0.20 to $-0.85V_{SCE}$ and recording the current density with time. Impedance spectra were recorded using a lock-in-amplifier*** from 100 MHz to 10 Hz and prior to collection of the EIS spectra, nickel was deposited on the Pt surface at $-0.75V_{SCE}$ for 25 sec.

The surface morphologies of the thin deposits were studied using scanning electron (SEM) microscopy using a field-emission SEM**** at an accelerating voltage of 4 kV. The crystallographic structures were determined using x-ray diffraction. An x-ray diffractometer† with fixed slit optics was used with a tube voltage of 30 kV and a tube current of 50 mA. A step scan of 0.02° and a dwell time of 3 sec were used for all measurements.

Results

Polarization curves for the two nickel electrolytes are shown in Fig. 1. Nickel deposition from the nickel sulfamate solution shows that nickel ion reduction commenced at about –0.70 to $-0.75V_{SCE}$. There was a small rise in current density between –0.40 to about $-0.55V_{SCE}$ followed by a steep increase in current density at $-0.70V_{SCE}$. Following this sharp rise in current density was a plateau at about $-0.73V_{SCE}$ and the current density again increased at $-0.76V_{SCE}$. Nickel reduction from the MSA solution also started at about $-0.70V_{SCE}$ followed by a rise in current density at $-0.75V_{SCE}$. A very small, less distinct plateau is seen at about $-0.76V_{SCE}$.

The impedance spectra seen in Fig. 2 show that the two nickel electrolytes exhibited different interfacial behaviors. Both exhibit slight inductance in the high frequency range (seen in the fourth quadrant) followed by the typical semicircle in the Nyquist plots. The nickel sulfamate electrolyte was slightly less resistive, 21.25 Ω, compared to the nickel methanesulfonate solution, 29.63 Ω. The major difference between the two nickel processes was the low frequency inductance seen in the nickel sulfamate process. Both electrolytes were modeled using simple circuit elements as seen in Table 1.

Potential step studies from the nickel solutions are seen in Figs. 3(a-d). A potential step of $-0.70V_{SCE}$ in the $Ni(CH_3SO_3)_2$ electrolyte showed an initial current density of ~4 mA/cm² (26 A/in.²), which then decreased with time. An E-step of $-0.75V_{SCE}$ resulted in a current density of about 8 mA/cm² (52 A/in.²), which slowly increased with time, reaching a minimum of 4 mA/cm² (26 A/in.²), then again increased to about 10 mA/cm² (65 A/in.²). An E-step of $-0.80V_{SCE}$ produced a similar I-time curve but the magnitude of the current density was slightly greater than that seen at $-0.75V_{SCE}$. Potential-steps in the sulfamate solutions resulted in similar current density-time transitions to those seen from the methanesulfonate

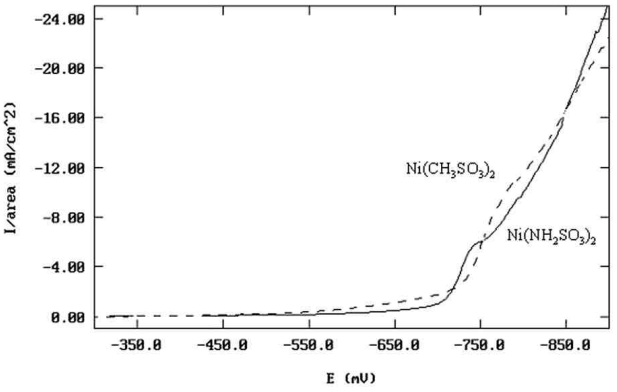

Figure 1—LSV curves for nickel methanesulfonate and nickel sulfamate showing onset of nickel plating.

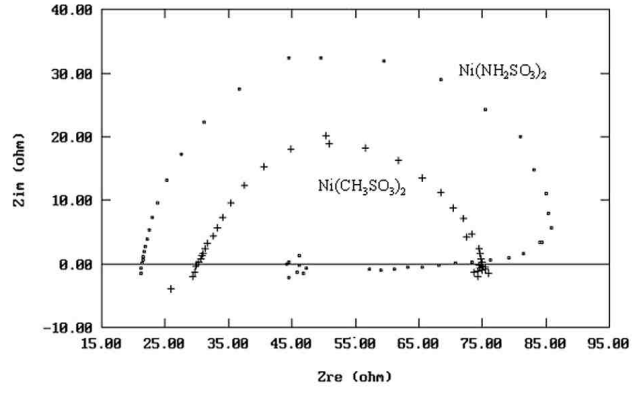

Figure 2—EIS spectra of nickel electrolytes revealing interfacial effects.

Table 1

Interfacial Circuit Elements for the Nickel Electrolytes

Circuit Element	$Ni(CH_3SO_3)_2$	$Ni(NH_2SO_3)_2$
L_1 (High Frequency, H)	5.94×10^{-6}	4.37×10^{-6}
R_1 (Solution Resistance, Ω)	29.63	21.25
R_2 (Interfacial Resistance, Ω)	45.43	58.10
Double Layer Capacitance (F)	5.3×10^{-5}	7.49×10^{-6}
Constant Phase Element	0.84	0.98
R_3 (Resistance Ω)	-----	54.38
L_2 (Low Frequency, H)	-----	13.05

*** EG&G PAR 273 potentiostat, Ametek - Princeton Applied Research, Oak Ridge, TN.*

**** EG&G 5210 High Performance Dual Phase Analog Lock-in Amplifier*

***** Leo 1530 field-emission microscope, Nano Technology Systems Division of Carl Zeiss SMT, Oberkochen (Germany).Cambridge (UK)/New York, NY.*

† Rigaku Ultima II, Rigaku/MSC, The Woodlands, TX.

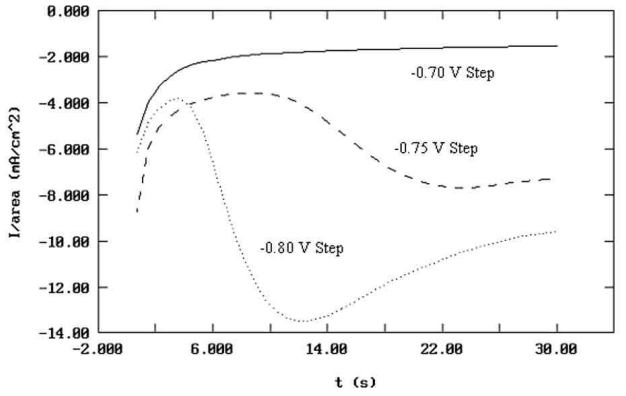

Figure 3(a)—Potential-step measurements in $Ni(CH_3SO_3)_2$ solutions.

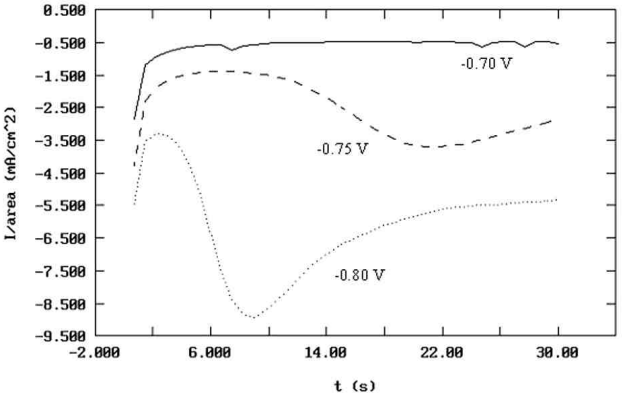

Figure 3(b)—Potential-sep measurements in $Ni(NH_2SO_3)_2$ solutions.

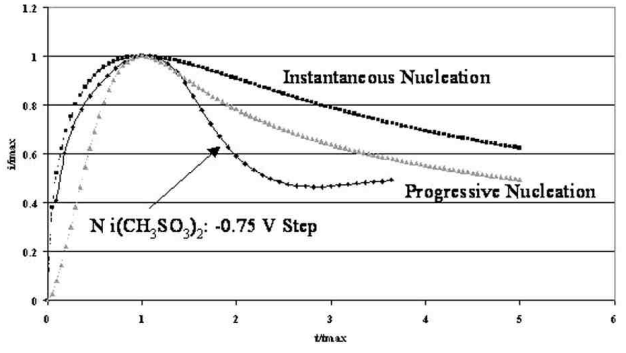

Figure 3(c)—Nucleation behavior of $Ni(CH_3SO_3)_2$ solutions step to Ð0.75V.

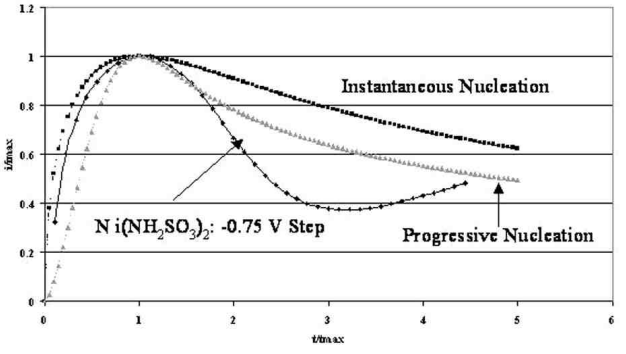

Figure 3(d)—Nucleation of nickel deposit from $Ni(NH_2SO_3)_2$ solution.

but the magnitude of the current density transitions was slightly less. At $-0.70V_{SCE}$, small fluctuations were seen in the I-time curve and at $-0.75V_{SCE}$ and $-0.80V_{SCE}$ the typical current-time-transitions (CTT) were seen.

Nucleation information extracted from the potential-step transitions is shown in Figs. 3(c and d). The dimensionless plots of i/i_{max} vs. t/t_{max} showed a sharp rise in i/i_{max} at short times, reaching a maximum at 1.0, which was then followed by a gradual transition

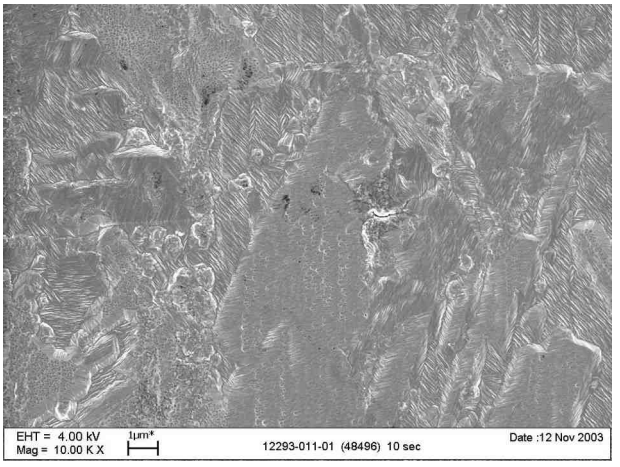

Figure 4(a)—SEM of $Ni(NH_2SO_3)_2$ coating after 10 sec of plating showing various grain structures.

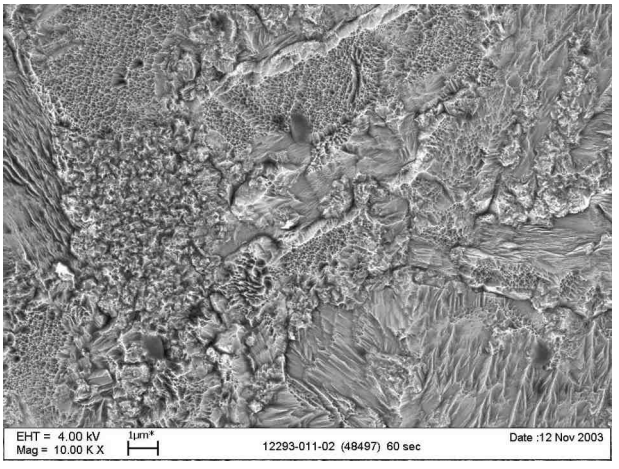

Figure 4(b)—$Ni(NH_2SO_3)_2$ coating after 60 sec of plating showing various grain structures.

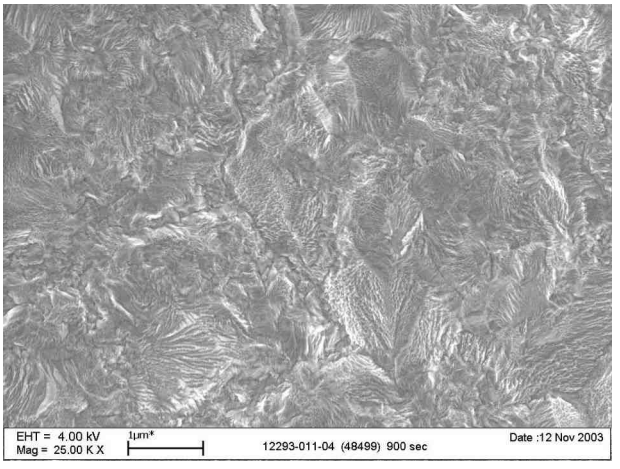

Figure 4(c)—$Ni(NH_2SO_3)_2$ coating after 900 sec of plating showing bulk grain structures.

to lower values. After reaching a minimum in i/i_{max} at about 2.5 to 3 in t/t_{max}, there was again a small increase in i/i_{max}.

SEM studies into the nickel deposit morphologies are seen in Figs. 4(a-c) and 5(a-e). The sulfamate deposits showed several morphologies such as fibers and rounded-mound structures in the very thin deposits. After 60 sec of plating, ~1 μm (~40 μ-in.) thick, the deposit continued to show various grain sizes and structures. Thick nickel sulfamate deposits were more uniform in morphology with a fibrous structure seen throughout the coating. Nickel deposits plated from the MSA solution on copper showed that the thin deposits (10 sec of plating, ~0.14 μm (~5.5 μ-in.) thick nickel) grew epitaxially on the copper substrate. There was evidence of twins or stacking faults in the nickel that were likely in the copper substrate originally. After 60 sec, there was still evidence of the epitaxy, as seen by the various grain structures and sizes in Fig. 5(b). After a thickness of about 1 to 4 μm (~40 to 160 μ-in.) nickel was deposited, the structure was influenced more by the composition of the plating electrolyte and deposition conditions rather than the underlying copper substrate. Faceting and a platelet-like morphology developed, as in Fig. 5(c). At longer times, the nickel grains coalesced and grew until they reached about 1 to 3 μm (~40 to 120 μ-in.) in size in the bulk nickel deposit.

XRD measurements made on the bulk (>25 μm (>0.001 in.) thick) deposits showed that both coatings exhibited the (100) orientation, as in Fig. 6. There was strong preferred orientation in both deposits.

Discussion

The chemistry of the nickel methanesulfonate process is similar in chemistry to that of the nickel sulfamate process. Both electrolytes showed an inhibiting effect at the onset of nickel crystallization but the degree of inhibition was slightly more pronounced in the sulfamate solution. Figure 1 shows that after the initial layer of nickel was deposited on the electrode surface, a plateau occurred

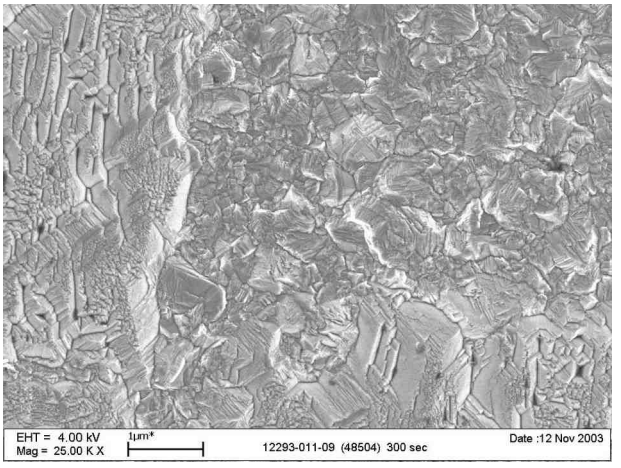

Figure 5(c)—Grain morphology in ~4-µm nickel coating plated from $Ni(CH_3SO_3)_2$ solution.

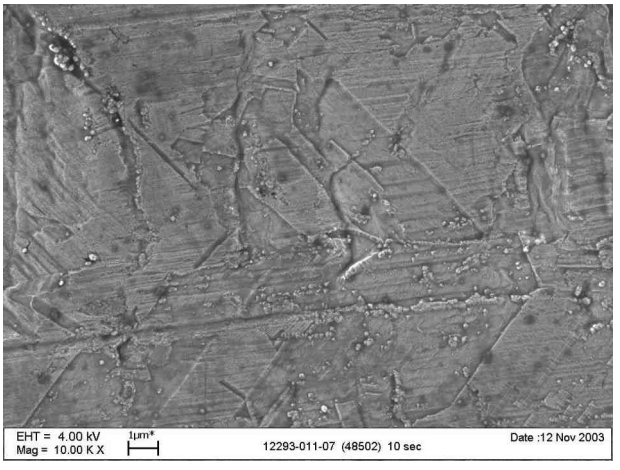

Figure 5(a)—Epitaxial nickel deposition on copper from the $Ni(CH_3SO_3)_2$ solution after 10 sec of plating.

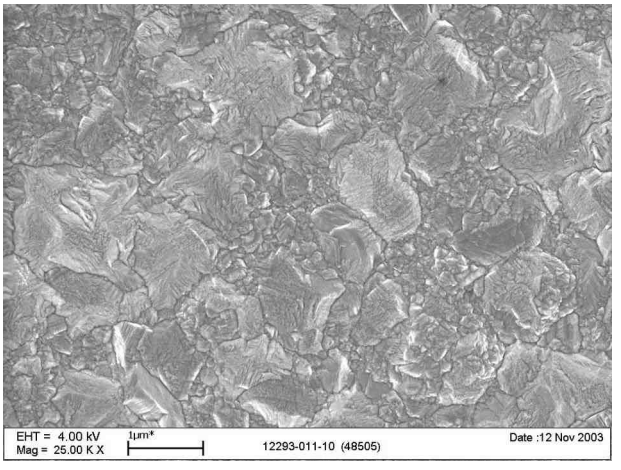

Figure 5(d)—Grain morphology in 12-µm nickel coating plated from $Ni(CH_3SO_3)_2$ solution.

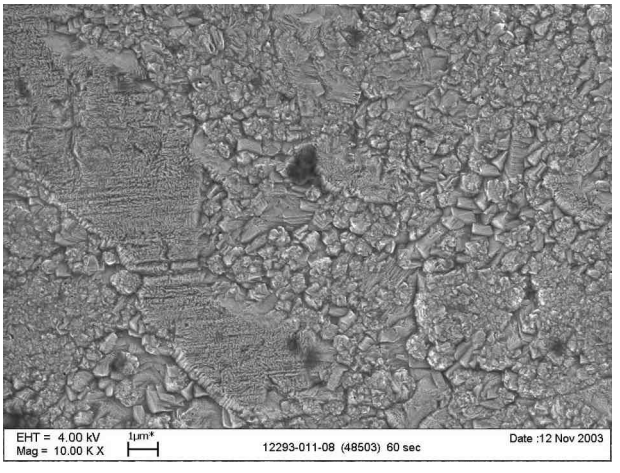

Figure 5(b)—Development of grain structure in nickel coating after 60 sec of deposition from the $Ni(CH_3SO_3)_2$ solution.

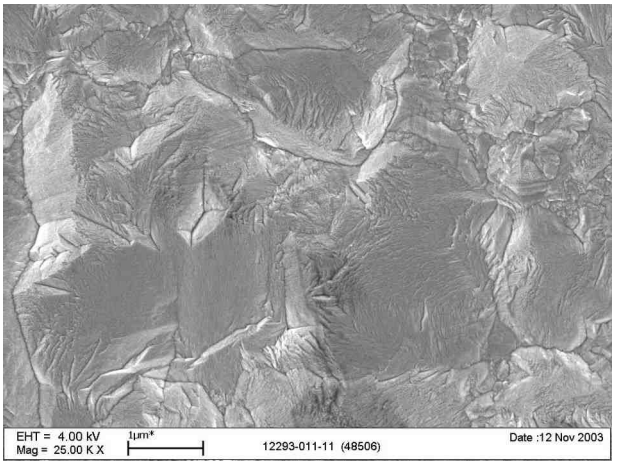

Figure 5(e)—Morphology of 25-µm nickel coating plated from $Ni(CH_3SO_3)_2$ solution showing gain growth.

in the sulfamate electrolyte, indicative of an adsorption process.[11] The polarization curve in Fig. 1 for the MSA process also showed a slight wave after the initial nickel coating was formed but not to the same extent as in the sulfamate curve. Further evidence of inhibiting effects is seen in the potential-step curves. The overall magnitude of the CTT curves was greater in the MSA solution than from the sulfamate electrolyte as these potential steps were chosen to correspond to the region where the inhibition in Fig. 1 was seen.

The impedance spectra in Fig. 2 confirm an additional circuit element in the low frequency region for the sulfamate process. For the methanesulfonate electrolyte, the circuit is modeled as $LR(RQ^n)$ and for the sulfamate process, $LR(RQ^n[RL])$[12] where:

L is an inductor,
R is the resistance,
Q is the double layer capacitance and
n is a constant phase element.

The solution resistance and charge transfer resistances were similar in both electrolytes. However, the double layer capacitance (C_{dl}) in the MSA solution was about 53 μF and while it was only 7 μF in the $NH_2SO_3^-$ solution. Loshkarev and Kryukova[13] showed a decrease in the capacitance of the double layer due to the adsorption of organic additives during tin plating forming a compact layer. The lower C_{dl} in the sulfamate solution, as compared to the MSA electrolyte, was likely due to stronger adsorption of the sulfamate anion (or its degradation products) contributing to the inhibition seen in Fig. 1. Also, the inductive effect in the low frequency region (4th quadrant) seen in Fig. 2 occurred only in the nickel sulfamate solution. Low frequency inductive behavior has been attributed to an adsorption process on the electrode surface.[14,15]

The stronger inhibition exhibited by the sulfamate anion, as compared to the methanesulfonate anion, manifested itself in changes in the deposit structures. The very thin deposits (<1 μm; <40 μ-in.), Figs. 5(a and b) show that the MSA deposit replicated the grain structure of the underlying copper (*e.g.*, grew epitaxially) whereas the sulfamate coating showed only slight evidence of the original copper structure, as in Figs. 4(a and b). The twins or stacking faults seen in Fig. 5(a) were copied from the underlying substrate. Nucleation and growth of the thin nickel coatings, as shown in Figs 3(c and d) appeared to follow an instantaneous growth process rather than one of progressive nucleation. Thirsk and Harrison[16] showed that the current for electrocrystallization of nuclei proceeds as follows:

$$I = nFC_oD^{½}/\pi^2t^2[1\text{-}exp(\text{-}N_oD(8\pi^3C_oV_m)^{1/2}t)]$$

for instantaneous nucleation, whereas for progressive nucleation, the current is:

$$I = nFC_oD^{½}/\pi^2t^2[1\text{-}exp(\text{-}4/3kN_oD(2\pi^3C_oV_m)^{1/2}t^2)]$$

where:

C_o is the concentration of Ni^{+2} in the bulk solution,
D is the diffusion coefficient,
V_m is the volume of material and
t is the potential pulse time.

Figs. 3(c and d) show that the very initial stages of nucleation from both electrolytes followed an instantaneous nucleation process. Instantaneous nucleation is shown schematically in Fig. 7(a). Discrete nuclei approximately the same sizes formed over the substrate and continued to grow if unimpeded, eventually forming a continuous layer. The rate constant for nickel ion reduction is:

$$\underset{Ni^{+2} + (2e^-)\ Substrate \rightarrow Ni^o\text{–}(M)}{k} \quad ; N(t) = N_o(1\text{-}(\exp kt))$$

where N(t) is the number of nickel nuclei formed at time t and N_o is the initial number of nuclei. For instantaneous nucleation, the rate constant, k, goes to infinity so the value of kt is much greater than one giving $N(t) \sim N_o$. After about 10 sec of deposition (corresponding to $t/t_{max} = 1$), there appeared to be a significant deviation from the instantaneous growth process changing to more progressive nucleation and growth (Fig. 7(b)). This change to progressive nucleation was reflected by a decrease in the rate constant, k, which went to zero and $kt << 1$ and therefore $N(t) \sim N_okt$. However, further deviation from progressive nucleation was seen and was likely due to nucleation and growth with significant edge effects as discussed by Bai and Conway[14] and shown in Fig. 7(c). Such edge effects in limiting growth of nuclei have been attributed to adsorption of organics around the edges of the nuclei, thus stunting their growth. The organic anions, $CH_3SO_3^-$ and $NH_2SO_3^-$, may have been adsorbed in the double layer as seen by the relatively low values of C_{dl} in Table 1. Previously, it was shown[17] that C_{dl} in organic-free tin electrolytes exhibited values of about 2000 $\mu F/cm^2$. The addition of organic grain refining additives to the tin solutions decreased C_{dl} to about 12 to 50 $\mu F/cm^2$. Thus, sulfamate and methanesulfonate anions in nickel solutions appear to behave similarly to organic grain refining additives, effecting the lateral and outward growth of the nickel coatings. Figs. 4(a and b) and 5(a and b) show several different grain structures and sizes that possibly arose from several electrocrystallization processes (*e.g.*, instantaneous, progressive and inhibited) occurring concurrently during nickel ion reduction.

After the deposit reached a thickness of about 3 to 5 μm (118 to 197 μ-in.), the copper substrate no longer exerted any influence on the deposit morphologies. Evidence of progressive nucleation is seen in Figs. 4(b) and 5(b). The grains in both bulk coatings were about 0.5 to 2 μm (20 to 79 μ-in.) in size, but

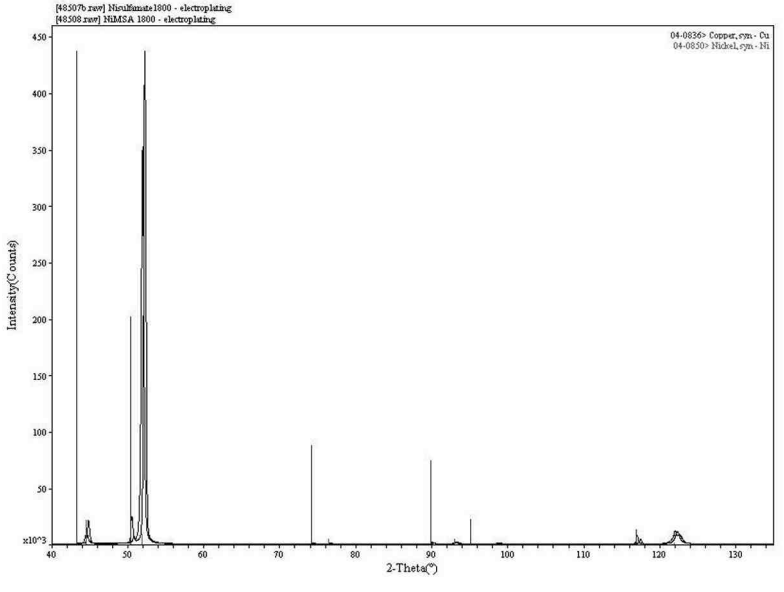

Figure 6—XRD Patters of $Ni(CH_3SO_3)_2$ and $Ni(NH_2SO_3)_2$ coatings showing (100) preferred orientations.

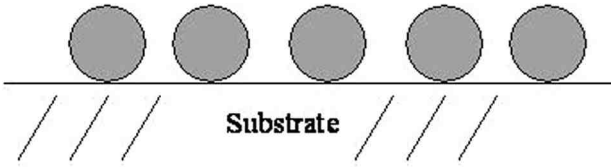

Figure 7(a)—Instantaneous growth mechanism [$N(t) = N_o \cdot (1-(\exp kt))$; $N(t) \sim N_o$ for all t].

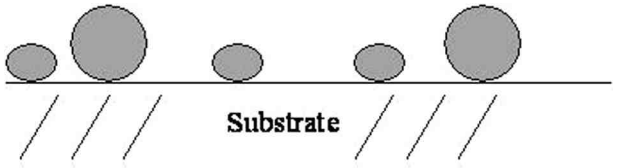

Figure 7(b)—Progressive nucleation growth process [$N(t) = N_o \cdot (1-(\exp kt))$; $N(t) \sim N_o kt$ for all t).

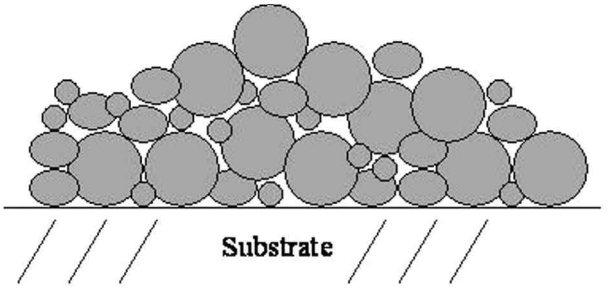

Figure 7(c)—Inhibited growth due to adsorption by organic anions.

the sulfamate coatings had a slightly overall smaller grain size due to the continuing inhibiting effect of $H_2NSO_2O^-$. The deposit structures were now influenced to a large measure by the chemistry of the plating solutions, pH and temperature (*e.g.*, inhibited growth). XRD measurements confirmed that the crystallographic structures of both coatings were identical.

Conclusions

Methanesulfonate appears to be an alternative electrolyte to sulfamate chemistries for nickel electrodeposition. Both electrolytes show inhibited nickel ion reduction but it is noted to a slightly greater extent in the sulfamate solution. The growth of the nickel coatings changes from an instantaneous process to a progressive one followed by inhibited growth because of the organic nature of the anions in solution. The structures of thick nickel coatings are similar as well.

References

1. M. Saleem, P.A. Borrk & J.W. Cuthbertson, *Electrochimica Acta*, **12**, 553 (1967).
2. N.V. Mandich & D.W. Baudrand, *Plating & Surface Finishing*, **89**, 68 (September 2002).
3. C. Coates, *Plating & Surface Finishing*, **75**, 26 (March 1988).
4. S. Kaja, H.W. Pickering & W.R. Bitler, *Plating & Surface Finishing*, **73**, 58 (January 1986).
5. S.H. Maron & A.R. Berens, *J. Amer. Chem. Soc.*, **72** (8), 3571 (1950).
6. C. Ho Huang, *Plating & Surface Finishing*, **81**, 64 (September 1994).
7. L. Jiazhu, Z. Haiyan & Z. Liangyu, *Plating & Surface Finishing*, **77**, 54 (July 1990).
8. N.M. Martyak, European Patent Application EP 0892087 A2 (1999).
9. V.N. Kudryavtsev, S.A. Maksimenko & I.S. Chernyshova, Proc. AESF SUR/FIN 1996, AESF, Orlando, FL, 1996; p. 837.
10. N.M. Martyak, US patent 5,944,879 A (1999).
11. R. Winand, in *Application of Polarization Measurements in the Control of Metal Deposition*, Elsevier, New York, NY, 1984; p. 133.
12. B.B. Boukamp, *Equivalent Circuit Users Manual*, University of Twente (1989).
13. M. Loshkarev & A. Kryukova, *Zhur. Fiz. Khim.*, **31**, 219 (1957).
14. L. Bai & B.E. Conway, *J. Electrochem. Soc.*, **138**, 2897 (1991).
15. L. Bai & B.E. Conway, *Electrochimica Acta*, **38** (14), 1803 (1993).
16. H.R. Thirsk & J.A. Harrision, *A Guide to the Study of Electrode Kinetics*, Academic Press, New York, NY, 1972.
17. A. Survila, Z, Mockus & S. Kanapeckaite, *Trans. IMF*, **80** (3), 85 (May 2002).

About the Author

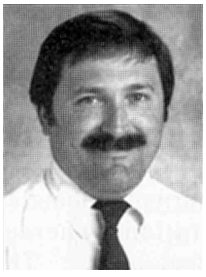

Dr. Nicholas M. Martyak, CEF, is a Senior Research Scientist at ATOFINA Chemicals, Inc., 900 First Avenue, King of Prussia, PA 19406. He holds a BS in chemistry from Cortland and was named a 2002 Distinguished Alumnus. He also has an MS in chemistry from the State University of New York, Binghamton, and a Ph.D. in materials science and engineering from Stevens Institute of Technology, Hoboken, NJ. He has been awarded nineteen patents with others pending and published over sixty journal articles.